Two-Dimensional Raman Spectroscopy of Vibrational Interactions in Liquids

A. Tokmakoff,* M. J. Lang, D. S. Larsen, and G. R. Fleming*
Department of Chemistry and The James Franck Institute, University of Chicago, 5735 S. Ellis Avenue, Chicago, Illinois 60637

V. Chernyak and S. Mukamel
Department of Chemistry, University of Rochester, Rochester, New York 14627
(Received 2 June 1997)

Two-dimensional fifth-order Raman spectroscopy has the ability to probe nonlinear interactions between well defined vibrational motions in liquids. It can reveal the nonlinear dependence of the molecular polarizability on vibrational coordinates, intermolecular interaction-induced effects, and anharmonic couplings between modes. We use this technique to probe these interactions at an intramolecular level in liquid CCl_4 and $CHCl_3$, and at an intermolecular level in a mixture of these two liquids. [S0031-9007(97)04158-6]

PACS numbers: 61.25.Em, 42.65.–k, 78.30.Cp, 78.55.Bq

One of the fundamental goals of the study of liquid dynamics is a molecular level description of the interactions between molecules as a basis for understanding physical properties and the rates of chemical reactions [1]. Liquid dynamics are inherently difficult to quantify on a molecular level due to the multiple time scales of intermolecular and intramolecular interactions. These manifest themselves as broadening of nuclear and electronic spectral signatures, thereby obscuring the details of the molecular interactions. The result of measurements on liquid dynamics in virtually all experiments is an ensemble-averaged two-point time-correlation function for liquid motions, or equivalently a spectral density or susceptibility [2]. This quantity generally lacks information on the nuclear coordinates or spatial dependencies of the dynamics, as indicated by the predominant use of the word "bath" to describe the modeling of the liquid in such experiments.

Moving beyond the traditional picture of the bath requires the use of structure-specific probes of molecular interactions. Furthermore, observables are required that can give multipoint correlation functions between different degrees of freedom, to quantify correlations or couplings between motions. Such requirements have been addressed in the field of nuclear magnetic resonance (NMR) in which two-dimensional (2D) spectroscopies allow such measurements to be made, although on a time scale which is slow compared to liquid dynamics [3]. In this Letter, we demonstrate the use of 2D vibrational spectroscopy which gives direct evidence of couplings between well defined motions within and between molecules in liquids. As in 2D NMR, 2D vibrational spectra are a powerful tool, giving qualitative information on couplings between well defined nuclear motions and elucidating coupling mechanisms through quantitative analysis. While the 1D Raman spectrum arises from polarizable vibrational modes of a sample, a 2D Raman spectrum has additional combination frequencies and cross peak features which are an indication of the couplings between modes.

The 2D vibrational technique presented here is a time-domain fifth-order nonlinear Raman spectroscopy [4]. This femtosecond nonresonant optical rephasing technique is related to the gated photon echo and Raman echo [5,6], and is meant to probe the low-frequency Raman spectrum ($1-700\ \mathrm{cm}^{-1}$). In condensed phases, intermolecular motions result in a broad and continuous spectral feature below $\sim 200\ \mathrm{cm}^{-1}$. A number of recent theoretical and experimental studies have demonstrated that 2D Raman spectroscopy can be used to probe heterogeneous dynamics underlying the low frequency spectral density [7–11]. When applied to discrete high-frequency intramolecular vibrations, the technique has the capacity to probe the nature of vibrational anharmonic couplings [12]. We show qualitative evidence of vibrational couplings here in 2D Raman spectra for two simple liquids, CCl_4 and $CHCl_3$, and a mixture of the two. These data give direct evidence of the strengths of interactions between well defined nuclear motions in a liquid. A discussion of the theory and a quantitative description is to follow [13].

The resonances in fifth-order Raman experiments result from multilevel coherences induced among all the possible vibrational levels. The fifth-order Raman pulse sequence and a representative diagram are shown in Fig. 1 [7,10]. A fs pulse pair excites Raman modes into coherence states $|a\rangle\langle b|$ at time t_0. These coherences evolve until a time t_2, at which time a second Raman interaction allows the initial coherence to be transferred to new coherences involving a third state $|c\rangle\langle b|$. The new coherence then evolves over a second period until it is probed at a time t_4. The existence of the fifth-order signal is an indication that coherent superpositions between the $|a\rangle$, $|b\rangle$, and $|c\rangle$ states can be formed.

Our microscopic analysis starts with the three-point polarizability correlation function that describes the response in the fifth-order experiment [4]

 0031-9007/97/79(14)/2702(4)$10.00

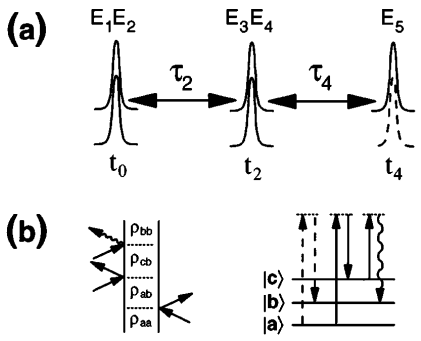

FIG. 1. (a) Pulse sequence and time variables for the fifth-order Raman experiment. (b) The primary rephasing double-sided Feynman diagram [5] and Lee and Albrecht ladder diagram [14] for an arbitrary three-level system.

$$R^{(5)}(\tau_2,\tau_4) = -\frac{1}{\hbar^2}\langle[[\tilde{\alpha}(\tau_4+\tau_2),\tilde{\alpha}(\tau_2)],\tilde{\alpha}(0)]\rangle,$$

where τ_2 and τ_4 refer to the time intervals between pulses. The natural reference model is a collection of harmonic oscillators where the polarizability $\tilde{\alpha}$ is linearly proportional to the vibrational coordinates q. For this model, the only nonvanishing response function is $R^{(3)}(\tau) = i\langle[\tilde{\alpha}(\tau),\tilde{\alpha}(0)]\rangle/\hbar$. All higher response functions such as $R^{(5)}$ vanish identically due to interference among Liouville space paths. We shall denote this model as "linear" since $R^{(3)}$ represents the linear nuclear response, although it is technically nonlinear in the radiation field. This suggests that there are two sources of nonlinearity, representing deviations from the reference model, which are responsible for $R^{(5)}$: nonlinear dependence of $\tilde{\alpha}$ on the nuclear coordinates and anharmonic couplings in the vibrational Hamiltonian [12].

The coordinate dependence of the polarizability is obtained by expanding $\tilde{\alpha}$ to higher order over all modes of the system

$$\tilde{\alpha} = \tilde{\alpha}(\mathbf{q}_0) + \sum_i \left(\frac{\partial\tilde{\alpha}}{\partial q_i}\right)_{\mathbf{q}_0} q_i + \tfrac{1}{2}\sum_{ij}\left(\frac{\partial^2\tilde{\alpha}}{\partial q_i\partial q_j}\right)_{\mathbf{q}_0} q_i q_j + \cdots$$
$$= \alpha^{(0)} + \alpha_i^{(1)} q_i + \alpha_{ij}^{(2)} q_i q_j + \cdots .$$

Within such an expansion, terms involving the second-order expansion coefficient $\alpha_{ij}^{(2)}$, which couple the q_i and q_j coordinates, will contribute to the fifth-order signal. More explicitly, a nonlinear dependence of the polarizability on the two coordinates leads to a fifth-order signal through correlation functions, such as

$$-\alpha_i^{(1)}\alpha_j^{(1)}\alpha_{ij}^{(2)}\langle[[q_i(\tau_2+\tau_4) \times q_j(\tau_2+\tau_4), q_j(\tau_2)], q_i(0)]\rangle/\hbar^2 .$$

This signal ($\alpha_{ij}^{(2)} \neq 0$) implies that the polarizability is nonadditive in both modes. The interaction with the radiation field then creates coherences among these modes which show up as mixed (cross) resonances. The cross ($i \neq j$) contributions to the polarizability arise either from intramolecular couplings through shared molecular electronic states, or from interaction-induced intermolecular couplings (local field effects) [15].

The second source of nonlinearity is vibrational anharmonicity [12]. Generally, for a ground state potential that includes a cubic anharmonicity of the form

$$V^{(3)} = \frac{1}{6}\sum_{ijk}\left(\frac{\partial^3 V}{\partial q_i\partial q_j\partial q_k}\right) q_i q_j q_k = g_{ijk}^{(3)} q_i q_j q_k ,$$

the fifth-order signal will have contributions proportional to $-\alpha_i^{(1)}\alpha_j^{(1)}\alpha_k^{(1)} g_{ijk}^{(3)}$. This anharmonic mechanism also allows the coupling of two states, but is distinct from electronic couplings in the nonlinear polarizability, since this is directly related to the liquid potential.

These two types of nonlinearities manifest themselves in the 2D fifth-order Raman experiment as the appearance of combination peaks in the spectral representation of the signal obtained by a 2D Fourier transform. We demonstrate this with simulations based on the Raman spectrum of CCl_4. Figure 2 shows the 1D polarized Raman spectrum of CCl_4 obtained by Fourier transformation of a fs nonresonant pump-probe experiment. The three underdamped C-Cl vibrational modes and the overdamped intermolecular contribution are modeled by a fit to four Brownian oscillator modes [5]. Figure 3 presents two simulations of the 2D fifth-order absolute value Raman spectrum of CCl_4 on the basis of this fit. This calculation shows a fifth-order response derived from the polarizability-induced nonlinearity $\alpha_{ij}^{(2)}$ and neglecting anharmonicities $g_{ijk}^{(3)} = 0$. The expressions for the 2D response were derived using the generating functions in Ref. [7]. The fit parameters from Fig. 2 were used as input. In Fig. 3(a) we assume a diagonal nonlinearity $\alpha_{ij}^{(2)} = \delta_{ij}$, i.e., an additive response in the four modes. The peaks along the frequency diagonals ($\omega_2 = \omega_4 = \pm\Omega_i$) are the peaks observed in the 1D spectrum. The only other features observed are the sum and difference frequency peaks that arise from the interaction of a vibrational coordinate with itself:

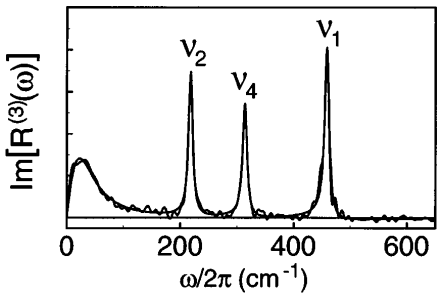

FIG. 2. The polarized Raman spectrum of CCl_4 taken from the sine transform of the 1D third-order Raman response $R_{ZZZZ}^{(3)}$. The spectrum has not been deconvolved. Also shown is a fit to three underdamped and one overdamped modes. The modes at 218, 314, and 460 cm^{-1} have relative amplitudes of 2.5, 3.0, and 7.1, and damping times of 1.2, 1.15, and 1.1 ps, respectively. The overdamped mode has an amplitude of 1.7 and exponential rise and decay times of 0.12 and 0.2 ps, respectively.

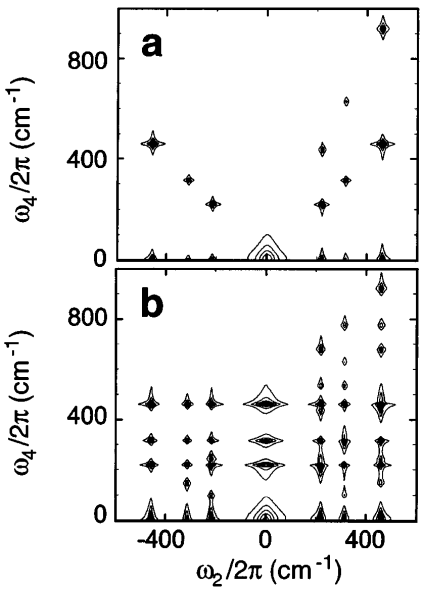

FIG. 3. Simulations of the 2D Raman spectrum $|R^{(5)}(\omega_2, \omega_4)|$ for CCl_4 between 0–700 cm^{-1} in two limiting cases. (a) Fully decoupled case ($\alpha_{ij}^{(2)} = \delta_{ij}, g_{ijk}^{(3)} = 0$) and (b) polarizability-coupled modes ($\alpha_{ij}^{(2)} = 1; g_{ijk}^{(3)} = 0$). Only two quadrants of the spectrum are shown, since the other two are equal by inversion symmetry.

the overtones ($2\omega_2 = \omega_4 = 2\Omega_i$) and zero-frequency peaks ($\omega_2 = \pm\Omega_i; \omega_4 = 0$). The ability of fifth-order experiments to probe the dephasing of overtones has been previously exploited [16]. Figure 3(b) shows a simulation including off-diagonal coupling through the polarizability $\alpha_{ij}^{(2)} = 1$, $g_{ijk}^{(3)} = 0$. The ability of the radiation field to create coherence between each of the modes leads to the appearance of various sum and difference frequency peaks, in addition to the features previously described for the decoupled spectrum. The placement of these combination peaks in ω_4 is correlated with the coupled fundamentals in ω_2 in a manner that makes assignment of the origin simple. Introducing anharmonicity as a form of coupling also leads to the same pattern of peaks as in Fig. 3(b), but now the relative amplitude of diagonal, cross-, and difference-frequency peaks for given modes in the spectrum can be used as an indication of the nature of the underlying nonlinearity.

To probe the existence of intramolecular and intermolecular interactions in simple liquids, 2D Raman spectra were obtained from fifth-order Raman measurements on CCl_4, $CHCl_3$, and a CCl_4:$CHCl_3$ mixture in a 1:1 mole ratio. To extract the fifth-order response $R^{(5)}(\tau_2, \tau_4)$, an intrinsic heterodyne detection geometry was used, which measures a cross term between the 1D and 2D signals $R^{(3)}(\tau_4)R^{(5)}(\tau_2, \tau_4)$, rather than the homodyne response $|R^{(5)}(\tau_2, \tau_4)|^2$ [17]. The heterodyne response was measured by sweeping both time variables in the correlation function in 16 fs steps for $\tau_2 = 0$ to 3 ps and $\tau_4 = 0$ to >2.2 ps. In all cases, the polarized response $R_{ZZZZZZ}^{(5)}$ was measured. $R^{(5)}(\tau_2, \tau_4)$ was obtained by dividing out the 1D third-order response contribution from the 2D data. Absolute value 2D spectra were obtained by 2D Fourier transformation of the data sets after truncating hyperpolarizability signals for $\tau_2, \tau_4 < 96$ fs and zero padding τ_2 and τ_4 to 8.2 ps. The resulting spectra shown in Fig. 4 are an average over two separate data sets, each of which were averaged over the slight uncertainty of the zero time and baseline of the third- and fifth-order responses. The process of dividing out the underdamped 1D response leads to the introduction of large uncertainties near the zero crossings. Although these uncertainties lead to distinct variations of the form of the signal, the spectral features in Fig. 4 are consistently present. Future acquisition of data from underdamped modes should consider the use of a heterodyne technique that measures $R^{(5)}$ directly rather than $R^{(3)}R^{(5)}$, although this is a more complex experiment than the one described here.

It is immediately clear from the data in Fig. 4 that there is strong evidence of cross (off-diagonal) nonlinearities between the intramolecular vibrational modes in these samples. In CCl_4 all three fundamental intramolecular vibrations observed show significant cross peaks between each other, as well as difference frequency peaks at points predicted by the simulation in Fig. 3(b). It is not surprising that a strong cross peak 1 ($\omega_2 = 460$ cm^{-1}, $\omega_4 = 219$ cm^{-1}) exists between the ν_2 and ν_1

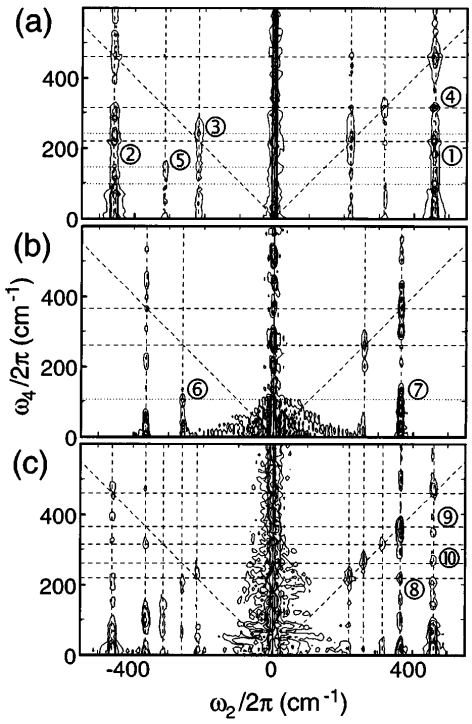

FIG. 4. 2D fifth-order Raman spectra $|R^{(5)}(\omega_2, \omega_4)|$ of (a) CCl_4, (b) $CHCl_3$, and (c) a 1:1 mole ratio CCl_4:$CHCl_3$ mixture. Labeled peaks are described in the text. Dashed lines show the fundamental frequencies, and dotted lines are difference frequencies.

modes, as a result of the Fermi resonance between $2\nu_2$ and ν_1. This coupling is also observed in the antidiagonal quadrant as a cross peak 2 ($\omega_2 = -460\ \mathrm{cm}^{-1}, \omega_4 = 219\ \mathrm{cm}^{-1}$) and as difference frequency peak 3 [$\omega_2 = -219\ \mathrm{cm}^{-1}, \omega_4 = (460-219)\ \mathrm{cm}^{-1}$]. A clear sign of coupling between the ν_4 and ν_1 modes is their cross peak 4 and the difference frequency peak 5 observed at [$\omega_2 = -314\ \mathrm{cm}^{-1}, \omega_4 = (460-314)\ \mathrm{cm}^{-1}$]. The intramolecular couplings in $CHCl_3$ are clearly much weaker, as evidenced by the significantly weaker cross peaks in Fig. 4(b). The only significant coupling features are the difference frequency peaks 6 and 7 between the 262 cm^{-1} ν_6 mode and the 368 cm^{-1} ν_3 mode [$\omega_2 = -\nu_6, \nu_3; \omega_4 = (\nu_3-\nu_6)\ \mathrm{cm}^{-1}$]. In both neat liquids, distinction between the two sorts of nonlinearity requires a quantitative analysis. This will be presented elsewhere [13].

Evidence for intermolecular interactions is present in the 2D spectrum of the CCl_4:$CHCl_3$ mixture in Fig. 3(c). The appearances of the cross peak 8 between the ν_2 mode of CCl_4 and the ν_3 mode of $CHCl_3$, peak 9 between the ν_1 mode of CCl_4 and the ν_3 mode of $CHCl_3$, and peak 10 between the ν_1 mode of CCl_4 and the ν_6 mode of $CHCl_3$ are clear indications of the coupling between the fundamental modes of the two molecules. The intermolecular cross peaks can be due either to anharmonic coupling of these coordinates on the collective liquid potential, or intermolecular interaction-induced effects which couple the fluctuations in the electronic states between molecules in the polarizability. Although these distinct mechanisms give rise to peaks at the same frequencies, they can be separated by the relative intensities of pairs of peaks in the spectrum [13]. In particular, the ratio in amplitudes of a coupling cross peak in the diagonal quadrant ($\omega_2, \omega_4 > 0$) to that in the antidiagonal quadrant ($-\omega_2, \omega_4 > 0$) can be used to determine the $\alpha_{ij}^{(2)}/g_{iij}^{(3)}$ ratio. In practice, two or three coupling elements, $\alpha_{ij}^{(2)}$ and $g_{ijk}^{(3)}$, can contribute to a given peak, but a self-consistent analysis of all peaks can extract unique values for each parameter in these tensor quantities.

The combination peaks observed in the 2D Raman spectrum are features that are directly related to the molecular description of the interactions that occur in liquids. Many features influence matrix elements for the cross peak amplitude, all of which give information on how different degrees of freedom in liquids interact. Careful investigation of these features can lead to important physical information such as the strength and time scales of interaction between polarizable electronic states, the symmetry of interactions among intermolecular and intramolecular motions, the role of interaction-induced effects, and dominant anharmonic couplings between vibrational modes. Quantifying these interactions for specific nuclear coordinates will help develop a molecular description of liquid dynamics. Although the overall time-correlation functions for solvent motions is reasonably well understood, 2D vibrational spectroscopy should allow a molecular description of the particular solvent motions involved in these relaxation processes. More generally, the technique of 2D vibrational spectroscopy is a powerful structure-specific tool that can be applied to static and dynamic correlation problems in condensed phases.

We thank Dr. Ko Okumura (Institute for Molecular Science) for discussions on the nature of couplings in the fifth-order experiment and sending preprints. We thank Xanthipe Jordanides for experimental contributions. This work was supported by a grant from the National Science Foundation, and a NSF Postdoctoral Fellowhip to A. T.

*Present address: Department of Chemistry, University of California, Berkeley, CA 94720.

[1] R. M. Stratt and M. Maroncelli, J. Phys. Chem. **100**, 12 981 (1996).
[2] G. R. Fleming and M. Cho, Annu. Rev. Phys. Chem. **47**, 109 (1996).
[3] R. R. Ernst, G. Bodenhausen, and A. Wokaun, *Principles of Nuclear Magnetic Resonance in One and Two Dimensions* (Oxford University Press, Oxford, 1987).
[4] Y. Tanimura and S. Mukamel, J. Chem. Phys. **99**, 9496 (1993).
[5] S. Mukamel, *Principles of Nonlinear Optical Spectroscopy* (Oxford University Press, New York, 1995).
[6] M. Berg and D. A. Vanden Bout, Acc. Chem. Res. **30**, 65 (1997).
[7] V. Khidekel and S. Mukamel, Chem. Phys. Lett. **240**, 304 (1995); V. Khidekel, V. Chernyak, and S. Mukamel, J. Chem. Phys. **105**, 8543 (1996).
[8] K. Tominaga and K. Yoshihara, Phys. Rev. Lett. **74**, 3061 (1995); J. Chem. Phys. **104**, 4419 (1996); **104**, 1159 (1996); K. Tominaga, G. P. Keogh, Y. Naitoh, and K. Yoshihara, J. Raman Spectrosc. **26**, 495 (1995).
[9] T. Steffen and K. Duppen, Phys. Rev. Lett. **76**, 1224 (1996); J. Chem. Phys. **106**, 3854 (1997).
[10] T. Steffen, J. T. Fourkas, and K. Duppen, J. Chem. Phys. **105**, 7364 (1996).
[11] A. Tokmakoff and G. R. Fleming, J. Chem. Phys. **106**, 2569 (1997).
[12] K. Okumura and Y. Tanimura, J. Chem. Phys. **106**, 1687 (1997); (to be published).
[13] A. Tokmakoff, M. J. Lang, D. S. Larsen, G. R. Fleming, V. Chernyak, and S. Mukamel, J. Chem. Phys. (to be published).
[14] D. Lee and A. C. Albrecht, Adv. Infrared Raman Spectrosc. **12**, 179 (1985).
[15] B. M. Ladanyi and Y. Q. Liang, J. Chem. Phys. **103**, 6325 (1995); B. M. Ladanyi and S. J. Klein, J. Chem. Phys. **105**, 1 (1996).
[16] K. Tominaga and K. Yoshihara, Phys. Rev. A **55**, 831 (1997).
[17] A. Tokmakoff, M. J. Lang, D. S. Larsen, and G. R. Fleming, Chem. Phys. Lett. **272**, 48 (1997).